

The BIPM 1.018 V Zener Measurement Set-up

by S. Solve, R. Chayramy, and M. Stock

Bureau International des Poids et Mesures
F- 92312 Sèvres Cedex, France



The BIPM 1.018 V Zener Measurement Set-up

S. Solve, R. Chayramy, and M. Stock
Bureau International des Poids et Mesures
F- 92312 Sèvres Cedex, France

Abstract. A new measurement set-up for calibration of secondary DC voltage standards at the level of 1.018 V has been developed by the Bureau International des Poids et Mesures (BIPM). A metrological validation process was developed to ensure the correct operation of the new set-up and to demonstrate its consistency with the previous set-up. Firstly, a direct comparison of two primary voltage standards shows that the voltage references are equivalent within their stated uncertainties. Secondly, two different methods were applied to compare the calibration results of five different Zener voltage standards obtained with the old and the new set-up.

All the results converge and confirm that the new automated measurement set-up is ready for operation. The new set-up is consistent with the previous system and metrological traceability to the previous Josephson voltage standard (JVS) is guaranteed.

1. Introduction

In the recent years, a new measurement set-up for calibration of secondary DC voltage standards at the level of 1.018 V has been developed by the BIPM Electricity Department [1]. The set-up allows the automated calibration of up to 12 Zener-based DC voltage standards against a primary voltage standard (a programmable array of Josephson junctions). In order to demonstrate metrological traceability of the results to the JVS, and to validate the replacement of the previous measurement set-up [2], we have carried out a significant number of experiments. The results and conclusions are presented in this report, which also includes a detailed technical description of the elements that constitute the new measurement system.

2. Equipment of the measurement set-up

2.1 The Programmable Array of Josephson Junctions

The heart of the primary DC voltage standard operated in the measurement set-up is a programmable array of 8192 Josephson SINIS (Superconductor/ Isolator / Normal Metal / Isolator / Superconductor) junctions (jj) produced by the PTB [3]. The array is divided into six cells with a total of 8173 operational junctions. The cells have been organized in the following sequence:

A- segment #1 : 7152 jj

B- segment #2: 512 jj

C- segment #3: 381 jj

D- segment #4: 8 jj

E- segment #5: 8 jj

F- segment #6: 112 jj

The segments were organized in this configuration because it is possible to achieve a total of 6744 junctions. When the set-up is biased with a suitable current issued from a programmable source (cf. §2.2) and irradiated with a RF signal of 73 Hz, the output voltage of the array will be exactly $U = 1.018\ 019\ 309\ 017\ \text{V}$ in terms of $K_{\text{J-90}}$.

Note: to achieve a total of 6744 junctions, segments #1 and #6 have to be biased in the positive polarity and segments #2 and #5 have to be biased in the negative polarity.

Note 2: a quick test to check for any trapped magnetic flux in the array can be carried out by opposing the voltages provided by segments #4 and #5. The result corresponds to the thermal electromotive forces (EMFs) along the measurement wires between the array at $T = 4.2\ \text{K}$ and at the laboratory temperature where the electrical connection to the measurement loop is performed. These EMFs are of the order of a few hundreds of nV and evolve linearly with time, as can be seen in figure 1. If Magnetic flux is trapped in the segments, it is mostly the case in the cells that contains less jj. Therefore, if this short test gives a result different from a null voltage, it would imply that magnetic flux has been trapped in the array.

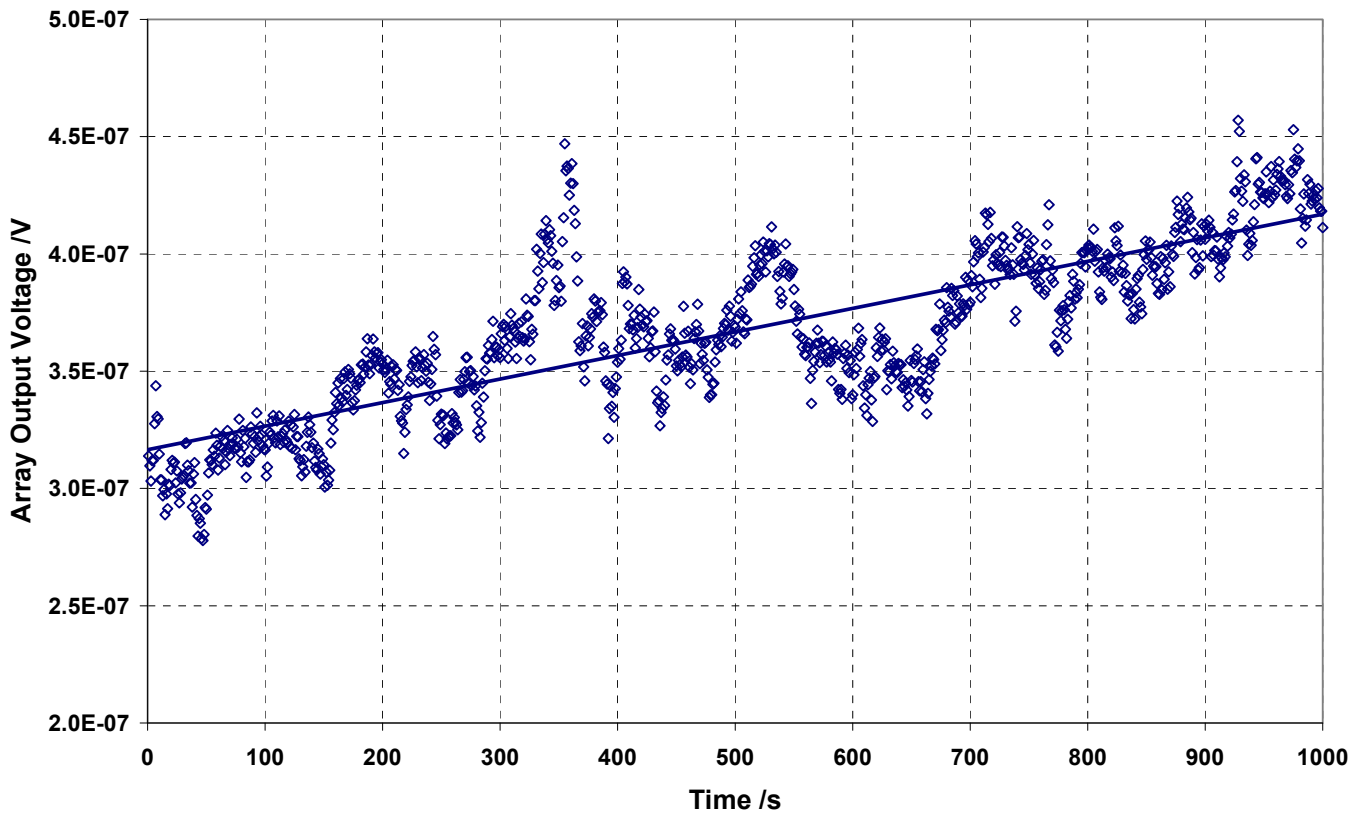


Figure 1: Temporal evolution of the output voltage of the SINIS array when two segments of 8 jj are biased in the opposite polarity.

A program written using Labview[®] software allows the operating point of each segment to be determined. The operating point corresponds to the biasing current value, which corresponds to the middle of the quantum voltage step. The program calculates an operating point for each polarity. For each segment, the operating points are stored in a text file (SEG*i*.dat) where “*i*” corresponds to the segment number. Figures 2a and 2b show the voltage response of each segment in terms of the corresponding biasing current. The Shapiro constant voltage steps are clearly visible and show a typical width of 2 mA.

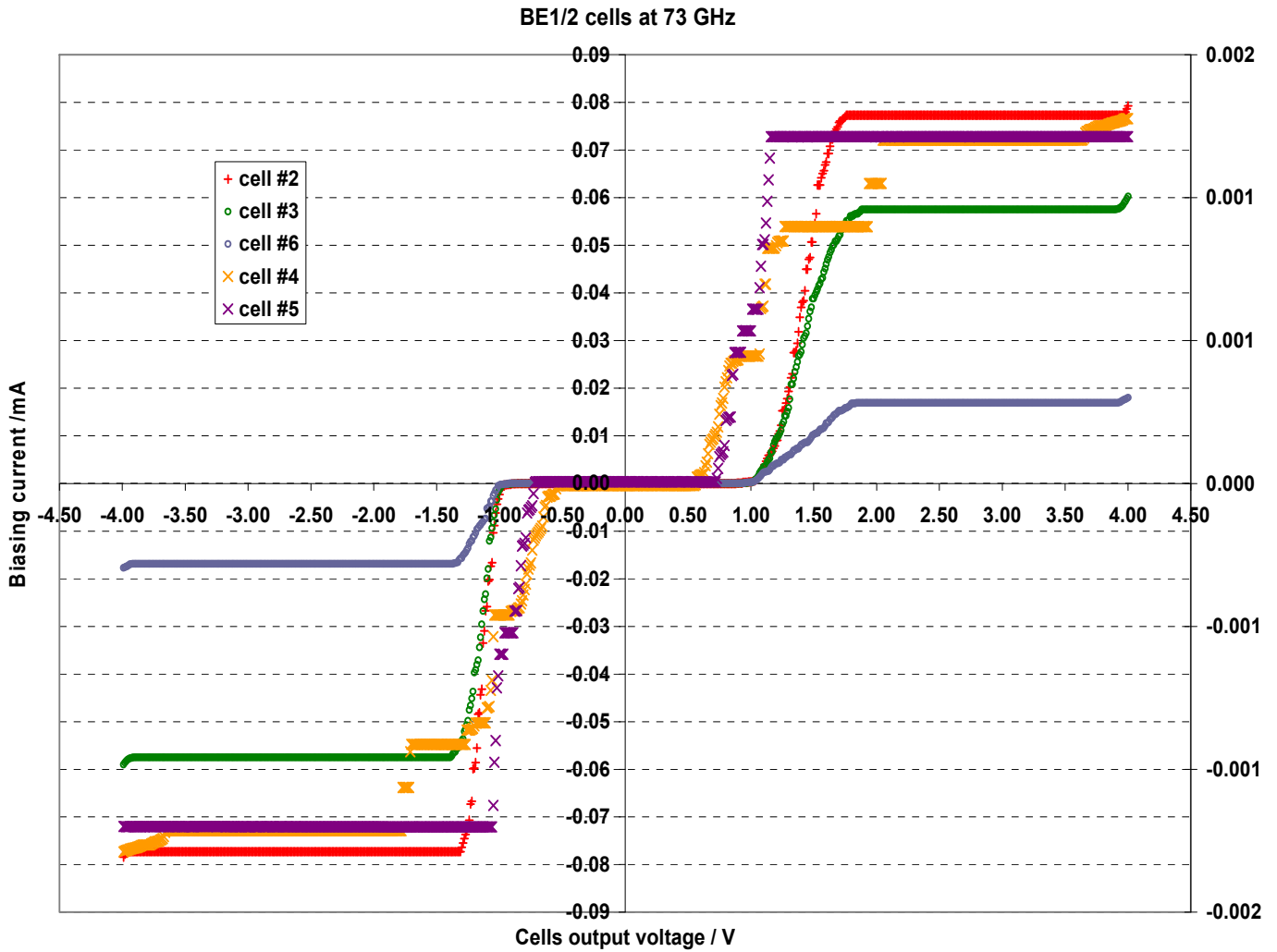


Figure 2a: Voltage response of 5 adjacent segments of the SINIS array operated in the 1.018 V calibration set-up. Segments #2 and #3 are referred to the left scale Y-axis and segments #4, #5 and #6 are referred to the right scale Y-axis.

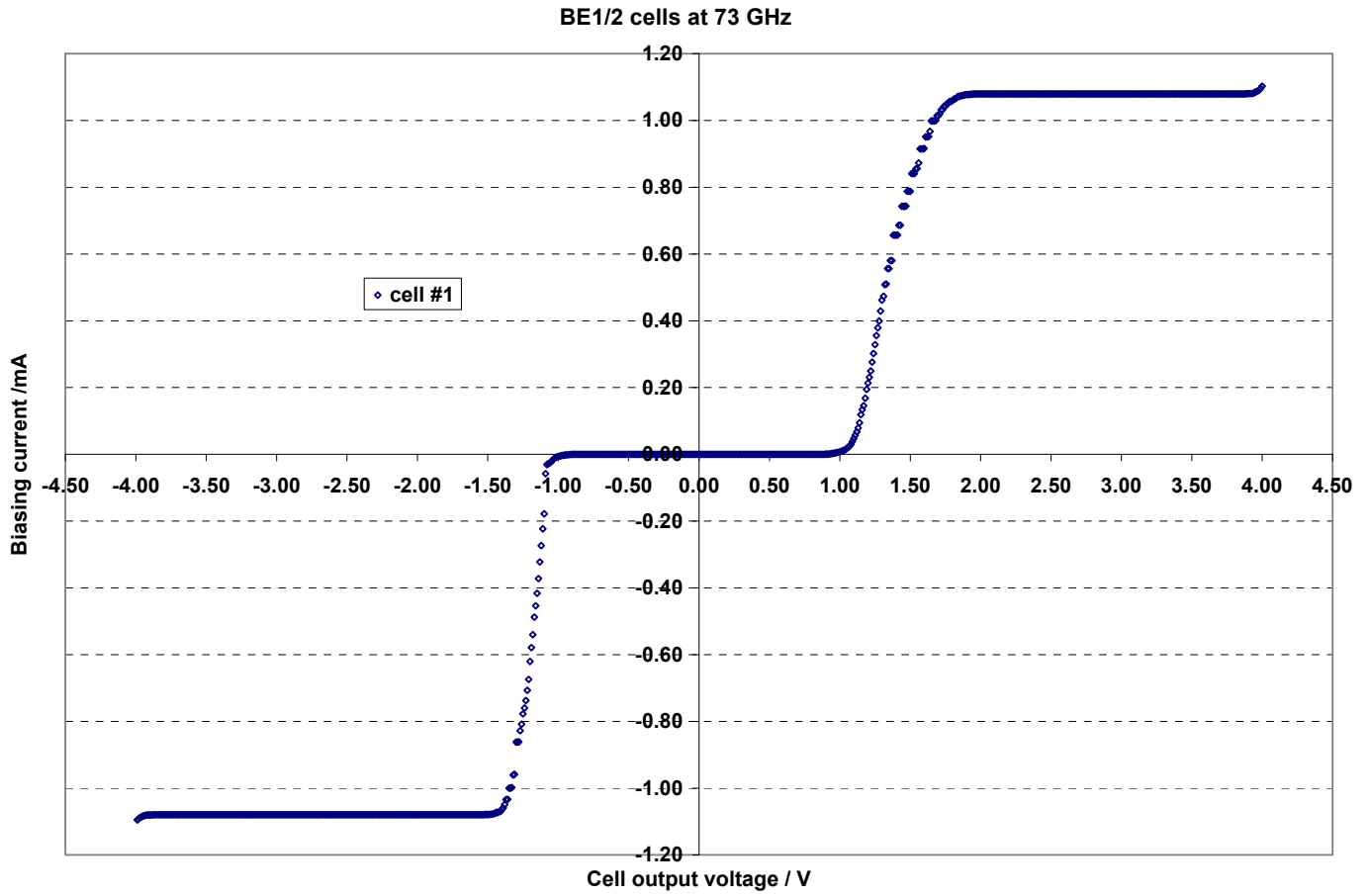


Figure 2b: Voltage response of the most significant segment of the SINIS array operated in the 1.018 V calibration set-up: segment #1 (7152 jj).

The dynamic characteristic of each segment of the array must be checked every time the calibration system is to be operated. This is because magnetic flux is likely to be easily trapped by programmable arrays.

A second program allows rapid setting of each segment to ON, that is to apply the current corresponding to the operating point (biasing current corresponding to the middle of the constant voltage step in one polarity and to reverse the polarity of the selected combination of the six segments (Fig. 2).

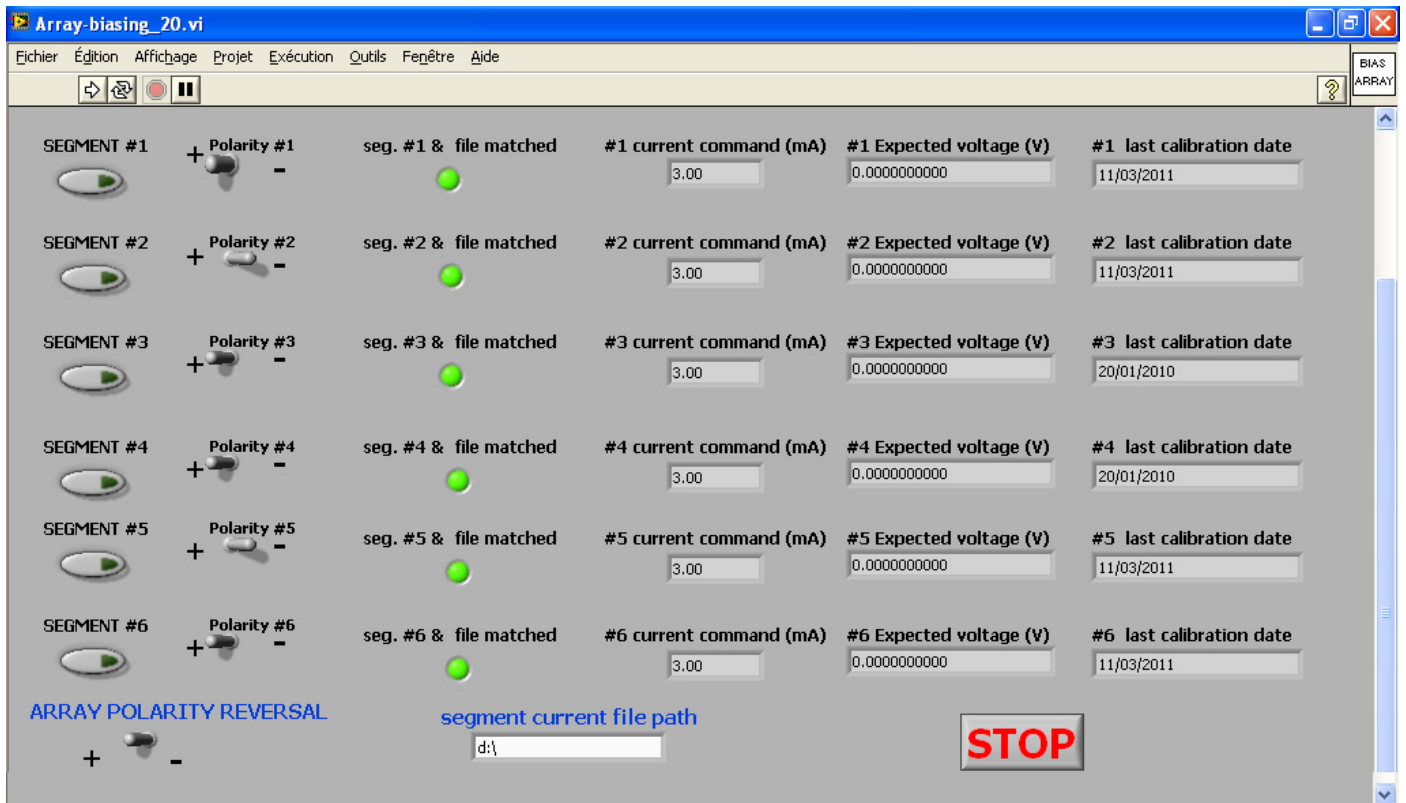


Figure 2: Front panel of the program used to bias the array in a defined configuration of the 6 segments.

Each segment is biased on its operating point (see the text for the definition).

Each line corresponds to one segment and contains: an ON/OFF switch; the polarity reversal switch; a boolean indicator that confirms the existence of the ASCII file containing the operating point value; its recorded value and the theoretical voltage. A final text file indicator shows the last date for the determination of the operating parameters.

2.2 Programmable Current Source

The current source is programmable and was built using a commercial 16-bit digital to analogue converter (DAC) board from which it is possible to use up to six voltage sources ranging from -10 V to $+10\text{ V}$. It was necessary to devise a way to isolate each output to independently bias six physically independent segments of the programmable array, because these sources are referenced to the same ground. This is done using an isolation amplifier for each array segment. The input of each isolation amplifier is powered with the same power supply but each output is powered with an independent power supply. The power supplies are all linear devices in order to avoid any electrical noise coming from the energy supply. A servo-controlled current gain loop located at each voltage output provides sufficient stability for the biasing of the segment of the array. The current range was set by selecting the values of the resistances R in the loop (Fig. 3a).

R was chosen to be equal to 1 k Ω in order to simplify the proportional coefficient between the voltage provided by the DAC and the resulting current in the segment. For instance, 4 V applied by the DAC will give a 4 mA current output. Fig. 3b shows the current stability of one of the programmable output sources.

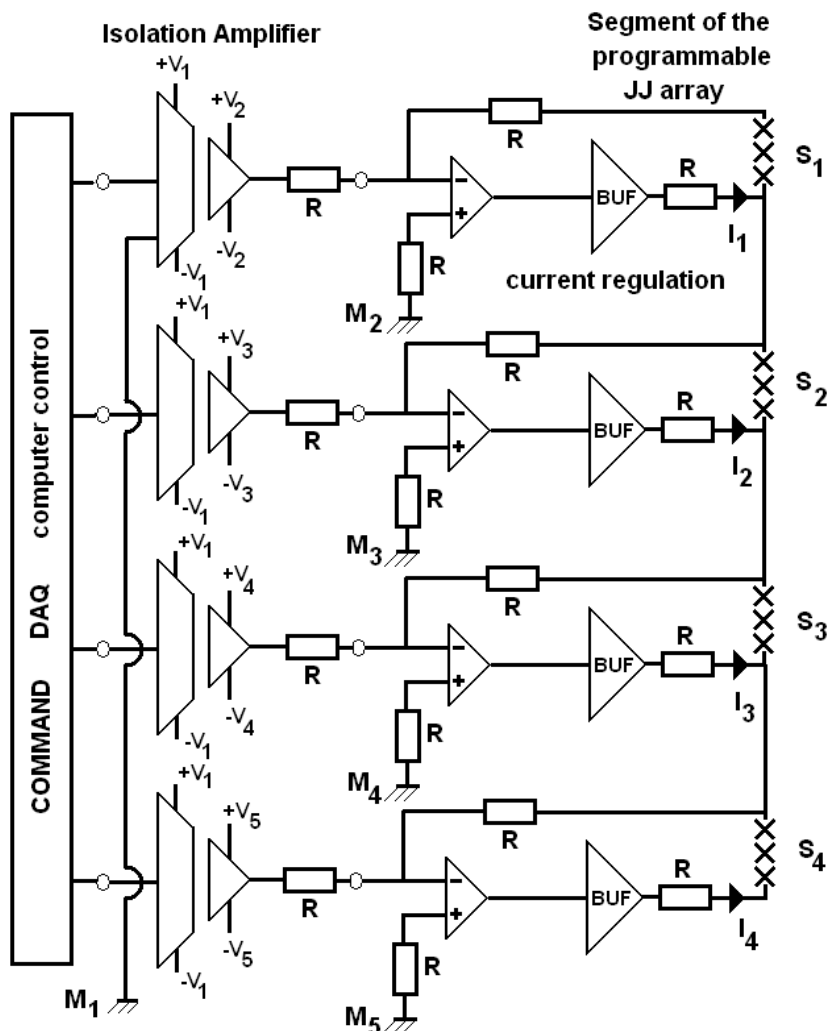


Figure 3a: Schematic of the bias source. The voltage provided by the DAC card is fed through an isolation amplifier and V/I converter.

The current source stability was investigated by recording the voltage across a 1 k Ω resistor that was fed by a current of 10 mA over 4 consecutive days. The results presented in figure 3b give a mean value of 9.984 mA associated with a simple standard deviation of the series of 0.01 mA. The difference of the mean value from 10 mA (0.016 mA) corresponds to the offset voltage of the isolation amplifier. This offset is stable and therefore can be compensated at the level of the voltage command sent to the DAC.

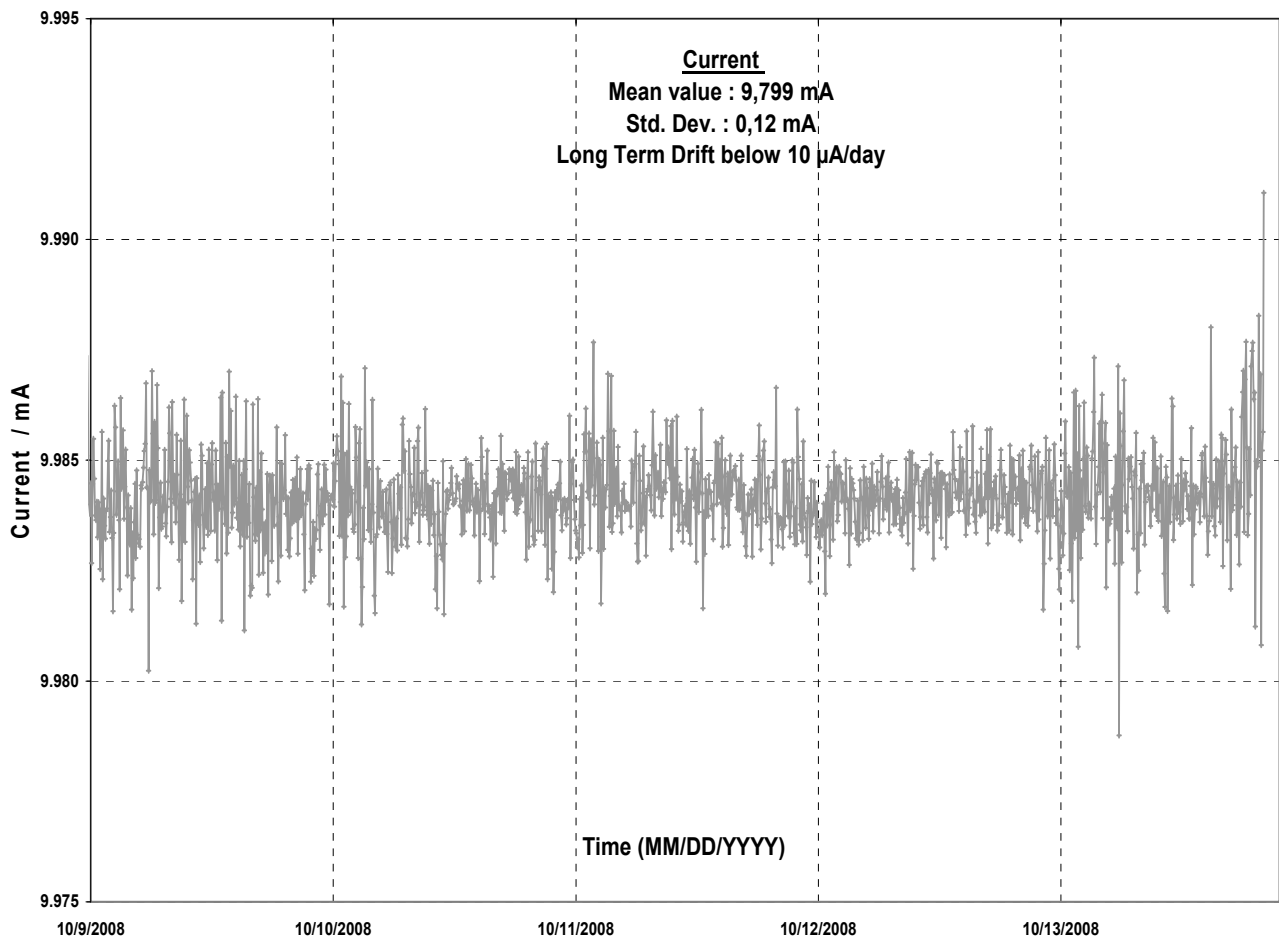


Figure 3b: Current stability of the biasing source for a current nominal value of 10 mA.

This bias source offers a great advantage in that it is possible to bias each segment independently on any of both polarities with no effect on the adjacent segments. Effectively, if all the sources were referred to the same reference potential, and if the requested voltage, for instance, was the voltage from segment one only, an exact opposite command would need to be sent to all the remaining segments, otherwise the current sent to segment 1 would circulate in the following segments, leading to additional undesired voltages.

2.3 Microwave source and waveguide

The compact microwave source that irradiates the array at $f=73$ GHz (Miniature Millimeter Wave Synthesizer) was fabricated by Jülicher SQUID GmbH in Germany. The waveguide is a 1.2 m PTFE waveguide with WR-12 flanges on each end. This equipment, which is no longer commercially available, has two main characteristics:

- a low loss of liquid helium: this is an advantage because the quantity of liquid helium required to run a programmable array is already larger than that needed to run a traditional hysteretic array, because the output voltage provided by the programmable array requires the circulation of a current within it.
- a high level of RF power attenuation of 3 dB: this is a disadvantage which was corrected by increasing the power level of the source at the top of the waveguide. The parameters of the installed RF amplifier were adjusted in such a way that the zero voltage Shapiro step and those of the first order are approximately the same width.

The RF source is referred to a 10 MHz signal provided by a generator, which is itself referred to the 10 MHz signal provided by the BIPM Time Department. The role of the RF generator is to allow an adjustment of the quantized output voltage without directly modifying the frequency of the compact synthesizer. The minimum frequency step of the RF source is 400 kHz, which corresponds to a voltage change of the order of 5.8 μV . It is possible to achieve a better resolution by changing the value of the 10 MHz reference signal*. As will be described in the calibration process, by using this technique it is possible to adjust the voltage reference to the output voltage of the secondary standard to within 100 nV and therefore to limit the amplitude of the error due to the detector gain.

It is possible to benefit from the use of an analogue detector (for example, EM N11) in the measurement set-up to measure the voltage difference, because the output voltage of the primary reference and that of the voltage standard to be calibrated are very close.

2.4 Programmable Multiplexer

For this system, we built a programmable multiplexer which provides the following electrical connections:

- selection of one of the twelve measurement channels for a Zener;
- polarity reversal of the Zener;
- polarity reversal of the detector;
- opening and closing of the measurement loop.

The device uses four rotary switches (*Electroswitch*) driven by stepper motors to select one of up to twelve Zeners per measurement (Fig. 4). A detailed description of the equipment will be submitted to a scientific journal [4].

* The frequency of the 10 MHz generator, f , is given by the formula : $f = \frac{U_z \times K_{J-90} \times 10}{73 \times 6744}$ where U_z is an estimation of the voltage of the Zener to be calibrated at the level of 10^{-7} .

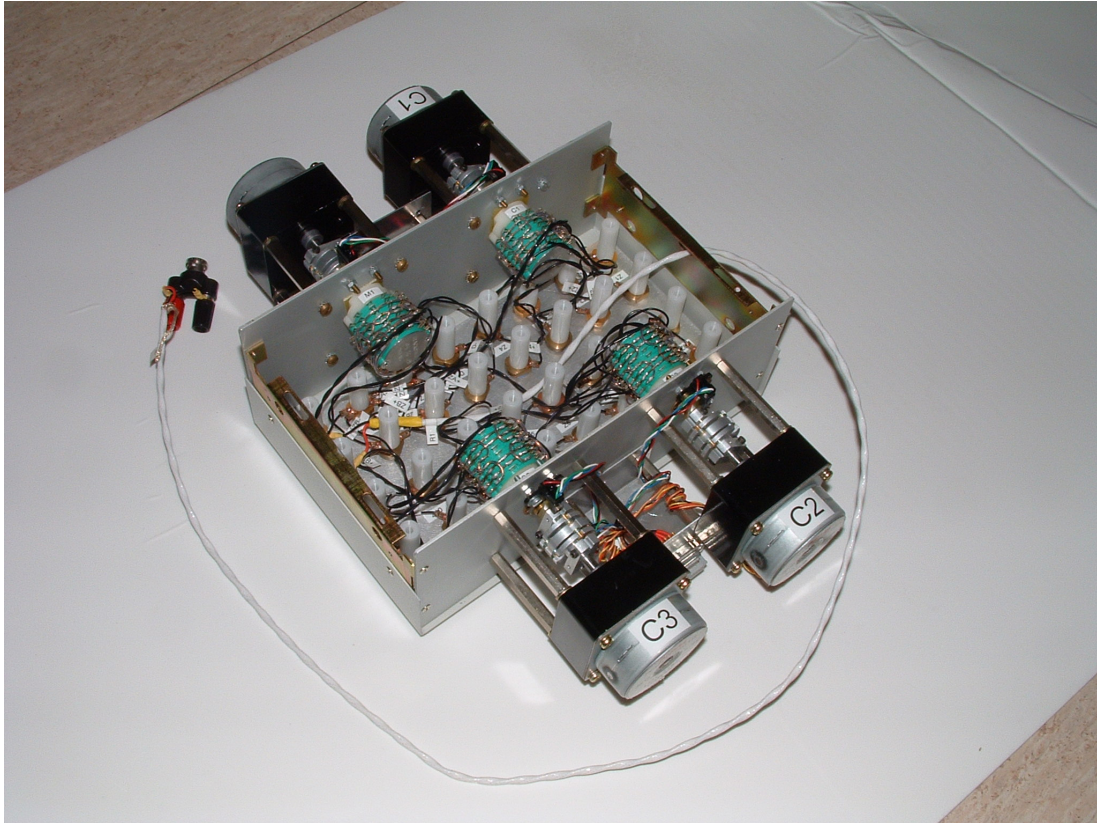


Figure 4: General view of the multiplexer. Note the four rotating switches that allow switching to different configurations.

The rotary switches feature high leakage resistance and very low thermal EMFs. The Zener voltage leads, the array leads and the output detector leads are all thermally anchored to the chassis inside the multiplexer (Fig. 5).

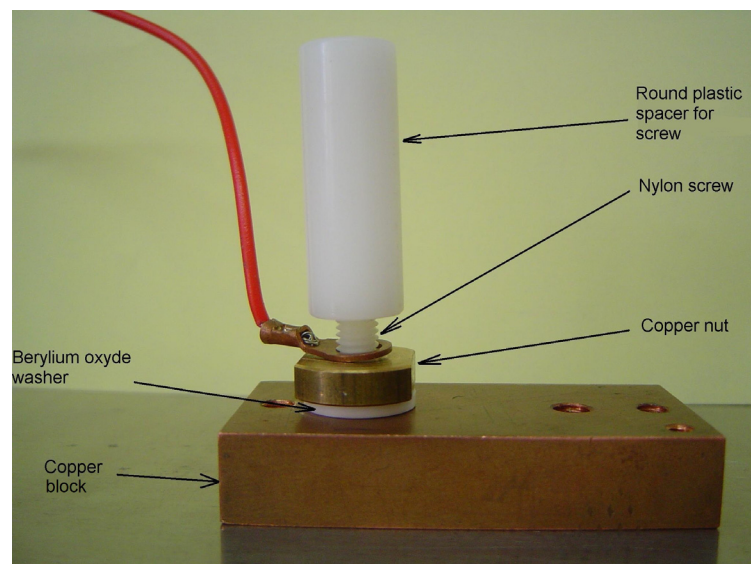


Figure 5: Detail of the thermal anchoring of the electrical connections inside the multiplexer.

Particular attention was paid to reduce to the minimum the amplitude of the residual thermal electromotive forces.

To reach this result, a combination of different techniques was used which are presented and illustrated below. Particular attention was paid to solder the copper wires to the switch contacts (silver) with a cadmium/tin alloy (70 %/30 %) [5].

The complete assembly shows a repeatability of the amplitude of residual thermal electromotive forces below 2 nV. Each rotary switch axis is coupled to a stepper motor through a coupling membrane (Fig. 6).

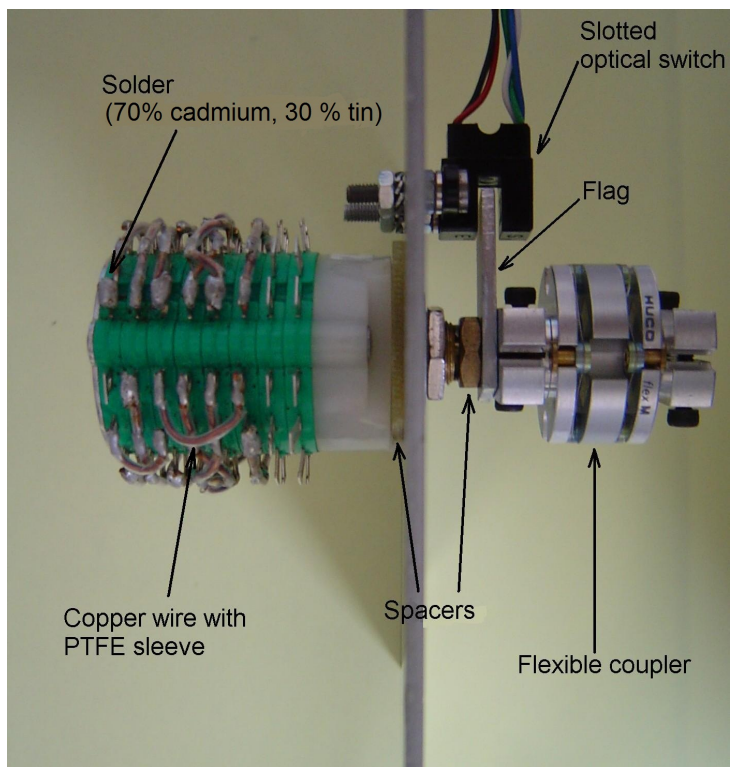


Figure 6: Structure of the rotating switch assembly.

A Digital Input/Output board (DIO) coupled to a data acquisition / switch unit provides an interface between the program and the motors (Fig. 7).

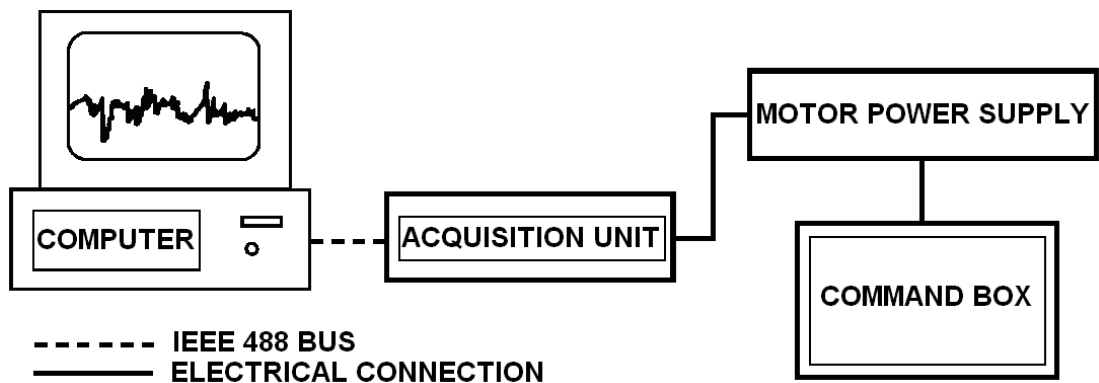


Figure 7: Organization of the instrumentation required to run the multiplex.

The motors are driven from a dedicated power supply which is shown in figure 8

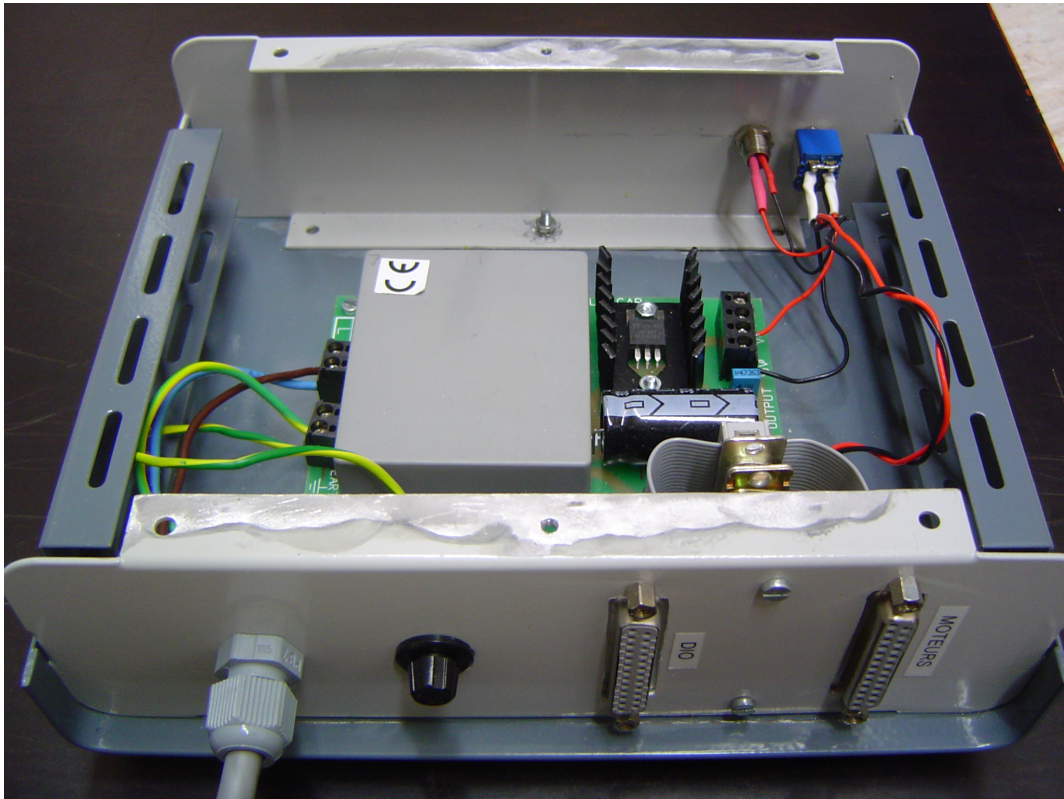


Figure 8: Picture showing the 12 V linear power supply used to drive the stepper motors.

All switch rotations are computer controlled via the DIO. The motor positions are re-initialized by using optical position detectors (Fig. 9) in order to keep track of the rotary switch positions in case of any accidental interruptions (software failure or power supply interruption). They also ensure that the motor and the rotary switch remain in phase during the measurement cycle.

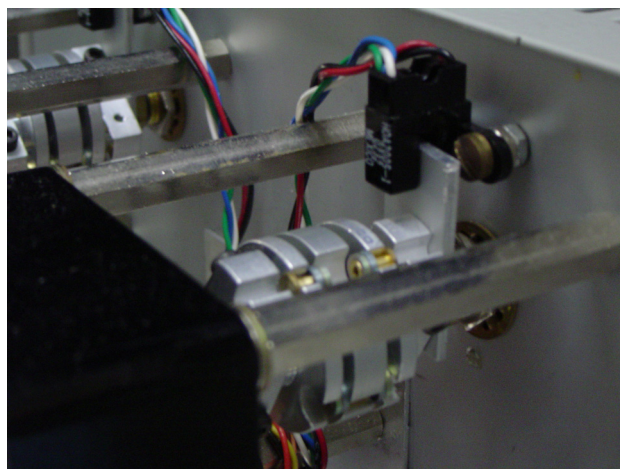


Figure 9: Detail of the optical detector used to initialize the rotary switch position.

The calibration of one Zener implies 11 sequential configurations of the multiplexer and corresponding orders sent to it:

- 1: selection of a Zener voltage reference, the detector is shorted and the Josephson array is biased.
- 2: The Zener and the Josephson array are connected together in series-opposition; the detector is connected to the measurement loop.
- 3: The detector polarity is reversed.
- 4: The detector polarity is reversed again to switch back to the configuration of step 2.
- 5: The detector is shorted and the measurement loop is opened (step 1)*.
- 6: The Zener and the Josephson array polarity are reversed.
- 7: The Zener and the Josephson array are connected together in series-opposition; the detector is connected to the measurement loop.
- 8: The detector polarity is reversed (step 3).
- 9: The detector polarity is reversed again to switch back to the configuration of step 2.
- 10: The detector is shorted.
- 11: The Zener is disconnected. The measurement loop is opened.

The multiplexer was built using components that have been designed to mechanically operate several tens of thousand of times without failure.

A series of 4096 consecutive measurements of a short-circuited channel of the multiplexer were performed, with an EM N11 analogue detector using its 3 μV range. The objective of the experiment was to evaluate the offset due to residual electromotive forces. The experiment lasted more than 36 hours and an Allan deviation with respect to the time was calculated from the series of measurements (Fig. 10).

* For a few seconds the Zener and the Josephson array are “in front of each other” and a small current might circulate from the array (low input impedance) to the Zener but this should not influence the measurements.

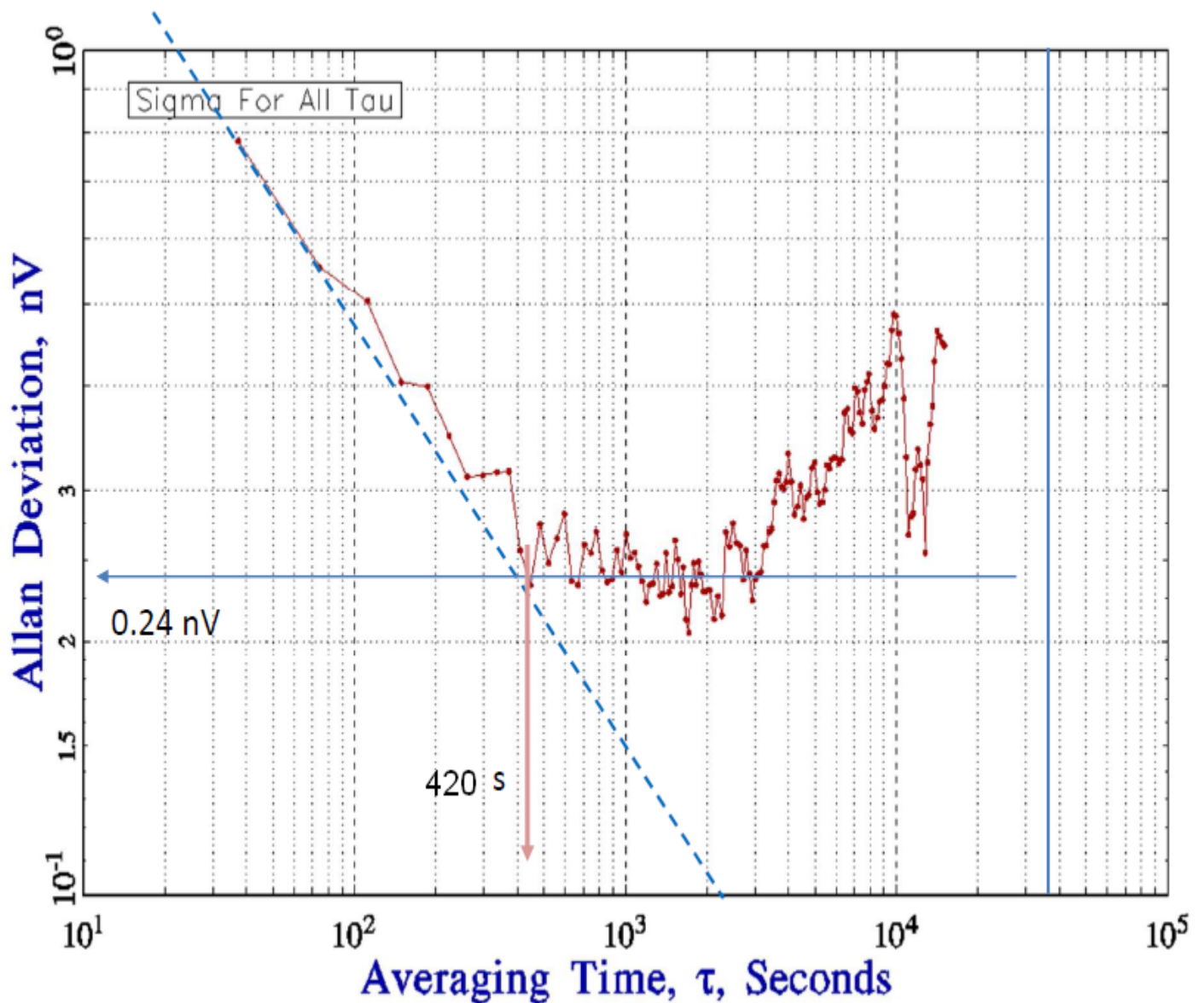


Figure 10: Allan deviation showing the 1/f noise floor of the multiplexer corresponding to 0.24 nV for an integrating time of 420 s.

The graph in figure 10 shows that the Allan deviation decreases linearly up to an integration time of 320 s, corresponding to a white noise regime. After 320 s, a 1/f noise floor of 0.24 nV is reached. This level is about 12.8 times greater than that expected from a shorted EM N11 [6] and therefore can be attributed to the electromotive forces limit attainable using the multiplexer. After 3000 s, the Allan deviation rises. This is interpreted as being caused by a periodic behaviour (period larger than 24 hours) probably related to temperature regulation in the laboratory.

3. Software and measurement process

3.1 Software

A program was written using Labview[®] software to perform all the operations required in the calibration process using an IEEE 388-2 communication interface. The device addresses appear on the front panel in such a way that they can be easily modified, if necessary.

The software allows the operator to create a list of the Zeners to be calibrated and eventually revise it (cancellation of some devices in the list or addition of others).

Time intervals can be adjusted by the operator to delay the beginning of the calibration process, to delay the acquisition sequence after a polarity reversal and to set the time interval between each nanovoltmeter reading.

For each set of readings, the software calculates the mean value, the median and the standard deviation of the series.

The number of readings is another parameter which can be adjusted.

The software sends the commands to perform the connections and the measurements. It provides information on the status of the calibration throughout the process and sends an email to the operator when the calibration is complete.

3.2 Measurement process

The behaviour of the array has to be checked (no trapped flux or bad RF coupling) and biased to the adequate voltage value before the start of calibration operations (*cf.* §2.1).

The following paragraph describes each step of the measurement process with its justification (if required).

- 1- The Zener to be calibrated is connected in series opposition with the array and the frequency of the 10 MHz reference of its RF synthesizer, f , is adjusted to bring the array voltage as closely as possible to the last calibration result U_Z of the Zener in accordance

with the formula:
$$f = \frac{U_Z \times K_{J-90} \times 10}{6744 \times 73}.$$

- 2- Measurement of the internal temperature of the Zener.

- 3- Both standards are set in their positive polarity and the reading sequence starts.
 - 4- The polarity of the nanovoltmeter that measures the voltage difference between the two standards is reversed and a reading sequence is carried out (the number of measurements is twice the number acquired in step 3).
 - 5- Both standards are set in their positive polarity again and the reading sequence starts.
- Note: the detector polarity is reversed to cancel out the offset and the internal thermal electromotive forces of the detector.
- 6- The detector is short-circuited, the measurement loop is opened, and the polarities of both standards are set to negative. This operation is performed through the multiplexer for the Zener and by reversing the biasing current on the Josephson voltage standard (JVS).
 - 7- The sequences 3, 4 and 5 are repeated in this polarity of the standards.
 - 8- The environmental parameters (P , T , RH) are measured.
 - 9- Measurement of the internal temperature of the Zener is repeated.

4. Results

In order to validate the metrological quality of this new measurement set-up and to ensure consistency with the present measurement set-up, we have carried out comparisons with different configurations of the two systems.

4.1 Direct comparison of the two primary standards

At the BIPM, the calibration of secondary standards has always been carried out against a primary standard (JVS). It was necessary to perform this operation manually because the detector for the measurement loop was an analogue nanovoltmeter measuring on its 3 μV range. Therefore, any step jump on the array would systematically lead to an overload of the detector. However, it was possible to automatically perform a calibration of a batch of 12 Zeners using a measurement loop based on a standard cell as the voltage reference*. The present JVS is based on a 10 V array of SIS (Superconductor / Isolator / Superconductor)

* As this process goes through the operation of a secondary voltage standard (standard cell), the results are considered as check results and not as calibration results even if the standard cell is calibrated against the primary voltage standard.

junctions which can, of course, also be set to the 1.018 V level. The first step was to investigate the quality of the new primary reference (“SINIS-based”) by comparing it to the “SIS-based” set-up. The individual results are presented in Figure 11.

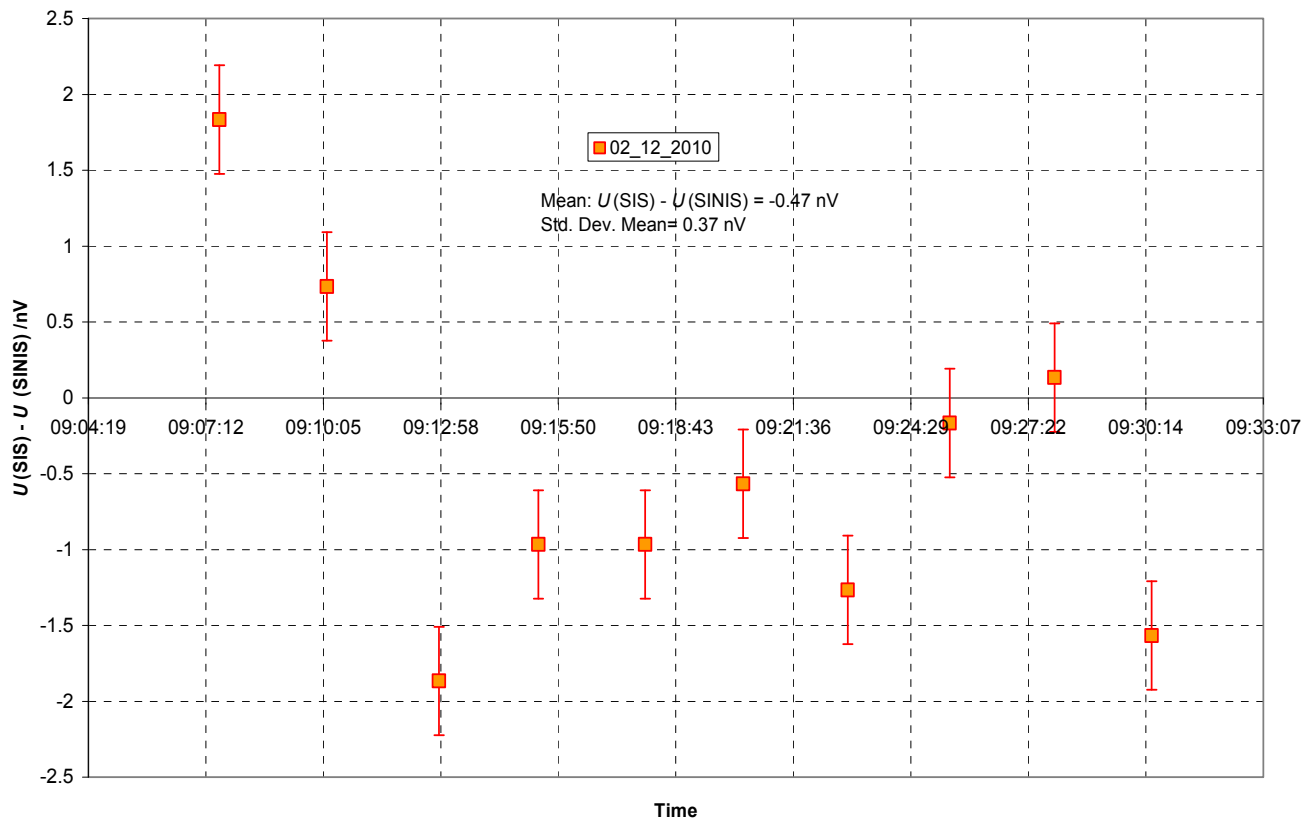


Figure 11: Results of the direct comparison of the two primary JVS involved in the BIPM Zener calibration set-ups.

The final result, $(U_{\text{SIS}} - U_{\text{SINIS}})$, is calculated as the simple mean of 10 individual measurements. Its associated repeatability (Type A uncertainty: u_A) is calculated as the standard deviation of the mean of the series:

$$(U_{\text{SIS}} - U_{\text{SINIS}}) = -4.7 \times 10^{-10} \text{ V with } u_A = 3.7 \times 10^{-10} \text{ V.}$$

The Type B uncertainties associated with the voltage difference between the two arrays are presented in Table 1. Details of the calculation of the components are given in the BIPM.EM-K10.b comparison reports [7].

	Type	Relative uncertainty	
		SIS	SINIS
Frequency offset	B	8.0×10^{-12}	1.0×10^{-10}
Leakage resistance	B	5.0×10^{-10}	7×10^{-10}
Detector	B	7.0×10^{-10}	
Total (RSS)	B	8.6×10^{-10}	7×10^{-10}

Table 1: Estimated Type B relative standard uncertainty components.

This comparison demonstrated that both standards agree very well within a total combined uncertainty of 11.7×10^{-10} V.

4.2 Comparison of the two set-ups through secondary voltage standards

4.2.1 Methodology

After the two primary standards were found to be equivalent, the BIPM became involved in the measurement of transfer standards through membership of a support group for the APMP.BIPM.EM-K11.3 comparison, to compare the results given by the two different set-ups.

Two BIPM Zener voltage standards (ZB and ZC) were selected for measurement, in addition to the three transfer standards (TZS-1, TZS-2 and TZS-3) for the APMP comparison.

Between 30 November 2010 and 10 December 2010, the 5 Zener voltage standards were calibrated alternatively with the two independent measurement set-ups. All the measurements were corrected for pressure and internal temperature dependence using the formula: $U_{Zcorr} = U_{meas} \cdot [1 + C_{th} \times (T_{ref} - T) + C_P \times (P_{ref} - P)]$, where U_{meas} is the Zener voltage measured, C_i are the correction coefficients, T_{ref} and P_{ref} the internal reference temperature and the pressure reference (atmospheric pressure) and T and P the internal temperature and the atmospheric pressure measured at the time of the Zener output voltage measurements.

The difference between the value attributed by the two set-ups to each Zener $d = (U_{\text{SINIS}} - U_{\text{SIS}})$, is computed using the least-squares fit at the mean time of the measurement period. The results are as follows:

$$d_{\text{TZS-1}} = -1.6 \text{ nV}, d_{\text{TZS-2}} = -4.2 \text{ nV}, d_{\text{TZS-3}} = -2.4 \text{ nV}, d_{\text{ZB}} = -11.8 \text{ nV}, d_{\text{ZC}} = +6.2 \text{ nV}$$

4.2.2 Uncertainty budget

The following list presents the uncertainty contributions of the Zener output measurements at 1.018 V.

(1) the Type A uncertainty due to the instability of the Zener; experience has shown that flicker or $1/f$ noise ultimately limits the stability characteristics of Zener diode standards and it is not appropriate to use the standard deviation divided by the square root of the number of observations to characterize the dispersion of measured values. For the present standards, the relative value of the voltage noise floor due to flicker noise is about 1 part in 10^8 . If the standard deviation of the mean of the results, σ_m , is smaller than the $1/f$ noise floor, the noise floor is taken as the Type A uncertainty. Table 2 presents the std. dev. of the mean obtained with the two set-ups.

	TZS-1	TZS-2	TZS-3	ZB	ZC
SINIS	8.8	7.5	10.7	6.9	6.3
SIS	9.3	6	4	5.5	5.8

Table 2: standard deviation of the mean of a series of 10 individual measurements of 5 Zeners with two different set-ups.

(2) the uncertainty due to the combined effects of the uncertainties of the pressure and temperature corrections calculated using the following assumption:

The uncertainty on the temperature correction due to the uncertainties of the temperature coefficients of each Zener standard is considered for the difference of the mean temperature over the whole measurement session from the reference temperature.

$$u_{\text{T-Zi}} = U \times u(c_{\text{T-Zi}}) \times \Delta R \text{ where } U = 1.018 \text{ V}, u(c_{\text{T-ZS1}}) = u(c_{\text{T-ZS2}}) = u(c_{\text{T-ZS3}}) = 0.29 \times 10^{-10} / \Omega, \\ u(c_{\text{T-ZB}}) = 0.52 \times 10^{-10} / \Omega, u(c_{\text{T-ZC}}) = 0.62 \times 10^{-10} / \Omega, \text{ and } \Delta R = 0.09 \text{ k}\Omega, \Delta R = 0.32 \text{ k}\Omega, \Delta R = 0.34 \text{ k}\Omega, \\ \Delta R = 0.09 \text{ k}\Omega, \Delta R = 0.34 \text{ k}\Omega, \text{ for TZS-1, TZS-2 TZS-3, ZB and ZC respectively.}$$

The same procedure is applied for the uncertainty on the pressure correction for the difference between the mean value of the pressure measured over the whole measurement session and the atmospheric pressure reference:

$u_{P-Zi} = U \times u(c_{P-Zi}) \times \Delta P$ where $U = 1.018 \text{ V}$, $u(c_{P-ZS1}) = u(c_{P-ZS2}) = u(c_{P-ZS3}) = 2.9 \times 10^{-10} / \text{hPa}$, $u(c_{P-ZB}) = 1.93 \times 10^{-10} / \text{hPa}$, $u(c_{P-ZC}) = 1.9 \times 10^{-10} / \text{hPa}$ and $\Delta P = (1013.25 - 998.4) \text{ hPa} = 14.9 \text{ hPa}$.

Note that the uncertainty on the measurement of the temperature and the pressure are negligible. The uncertainty contributions from temperature and pressure corrections are presented in the following table for each Zener.

Uncertainty / nV	TZS-1	TZS-2	TZS-3	ZB	ZC
Temperature correction / nV	2.6	9.3	9.9	4.7	13
Pressure correction / nV	4.3	4.3	4.3	2.9	2.8

Table 3: contributions of the temperature and pressure corrections for each Zener investigated in nV.

(3) the uncertainty component arising from the realization of the volt at the BIPM; this component is correlated for the five Zener standards and is presently equal to 0.9 nV.

Table 4 summarizes the uncertainties related to the calibration of a Zener diode against the two different measurement set-ups based on two different Josephson array voltage standards.

Uncertainty Component	Type	Contribution for the SIS system /V	Contribution for the SINIS system /V
Noise in the meas. loop	A	$3,4 \times 10^{-9}$	5×10^{-9}
Nanovoltmeter accuracy	A	$1,1 \times 10^{-10}$	$1,1 \times 10^{-10}$
Zener noise	A	Depending on the Zener but $\geq 10 \times 10^{-9}$	Depending on the Zener but $\geq 10 \times 10^{-9}$
Internal temperature and atmospheric pressure correction	B	Depending on the Zener Typically 10×10^{-9}	Depending on the Zener Typically 10×10^{-9}
Frequency stability of the RF source (JVS)	B	8×10^{-12}	1×10^{-10}
Leakage resistance on the meas. leads of the JVS.	B	5×10^{-10}	7×10^{-10}
Total (RSS)- typical		14.6×10^{-9}	15×10^{-9}

Table 4: Typical uncertainty budget for the calibration of a Zener against a BIPM primary voltage standard. Two measurement set-ups (one based on a SIS array, the other on a SINIS array) are presented.

4.2.3 Measurement results

The results obtained with the two measurement set-ups for the five Zeners that were calibrated are presented in the following figures (Figs. 12a, 12b, 12c, 12d and 12e).

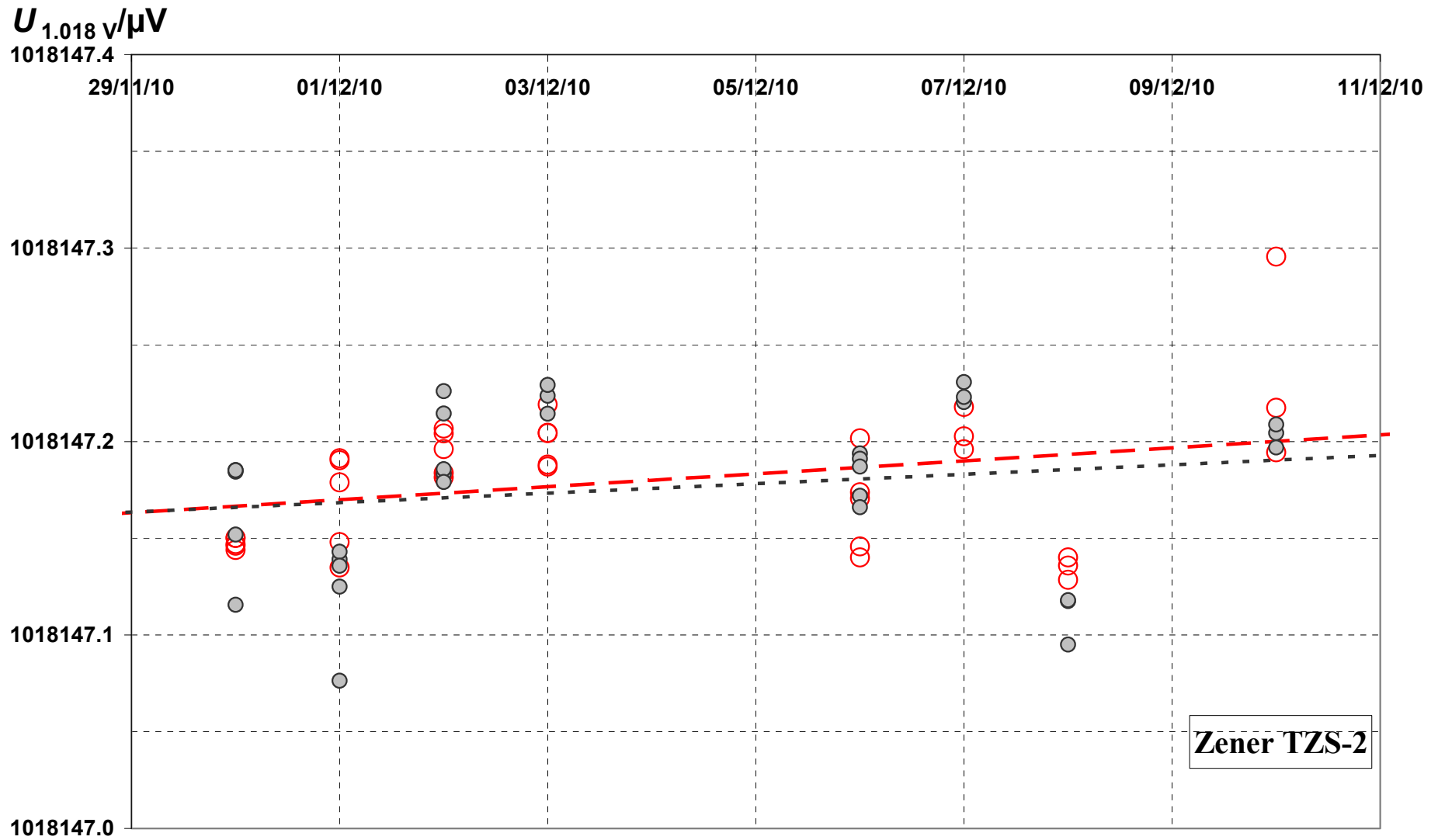


Fig. 12b : Day to day measurement result of TZS-2: the grey disks are the points obtained with the SINIS-based system and the open circles are the points obtained from the SIS-based system.

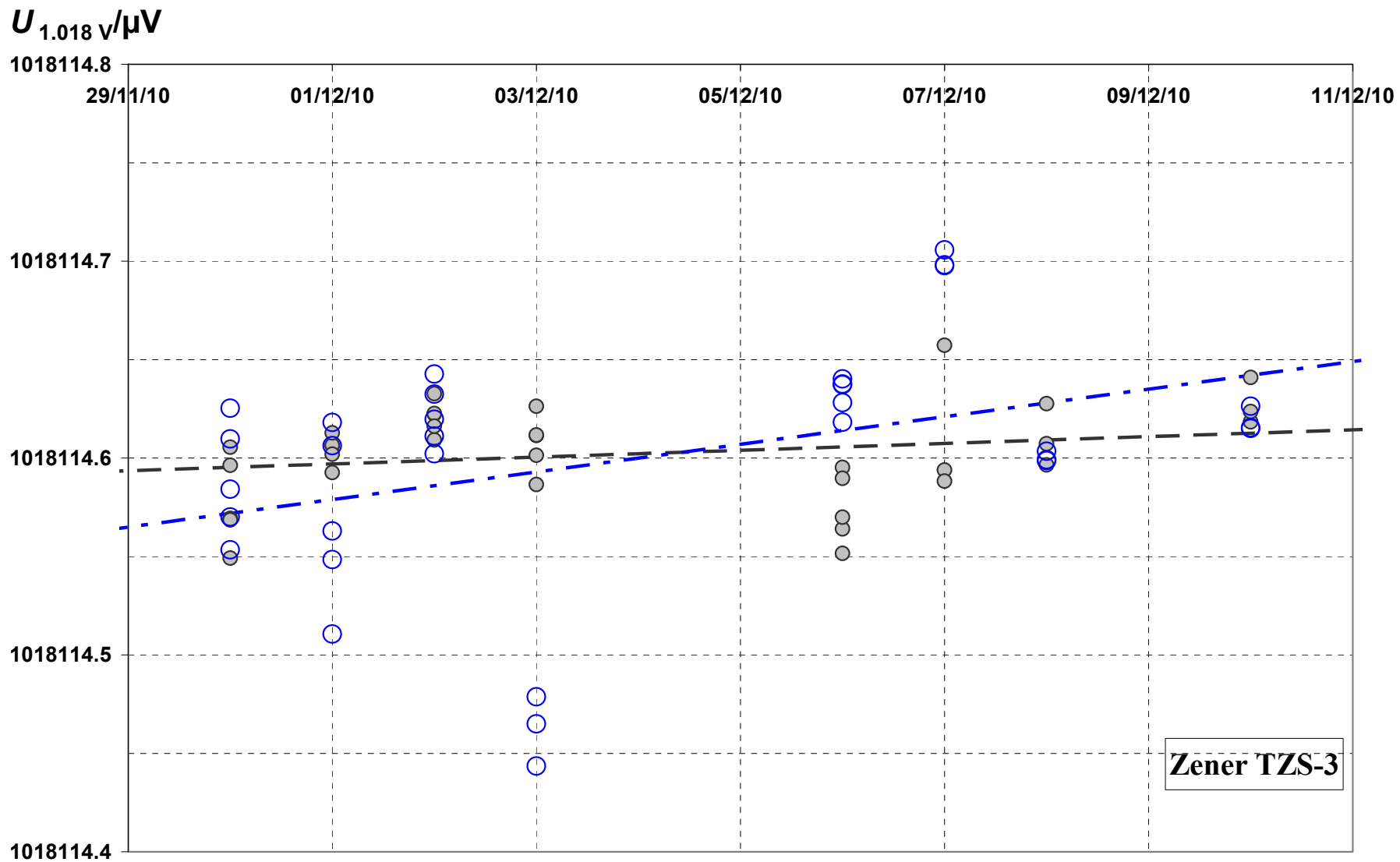


Fig. 12c : Day to day measurement result of TZS-3: the grey disks are the points obtained with the SINIS-based system and the open circles are the points obtained from the SIS-based system.

$U_{1.018 \text{ V}/\mu\text{V}}$

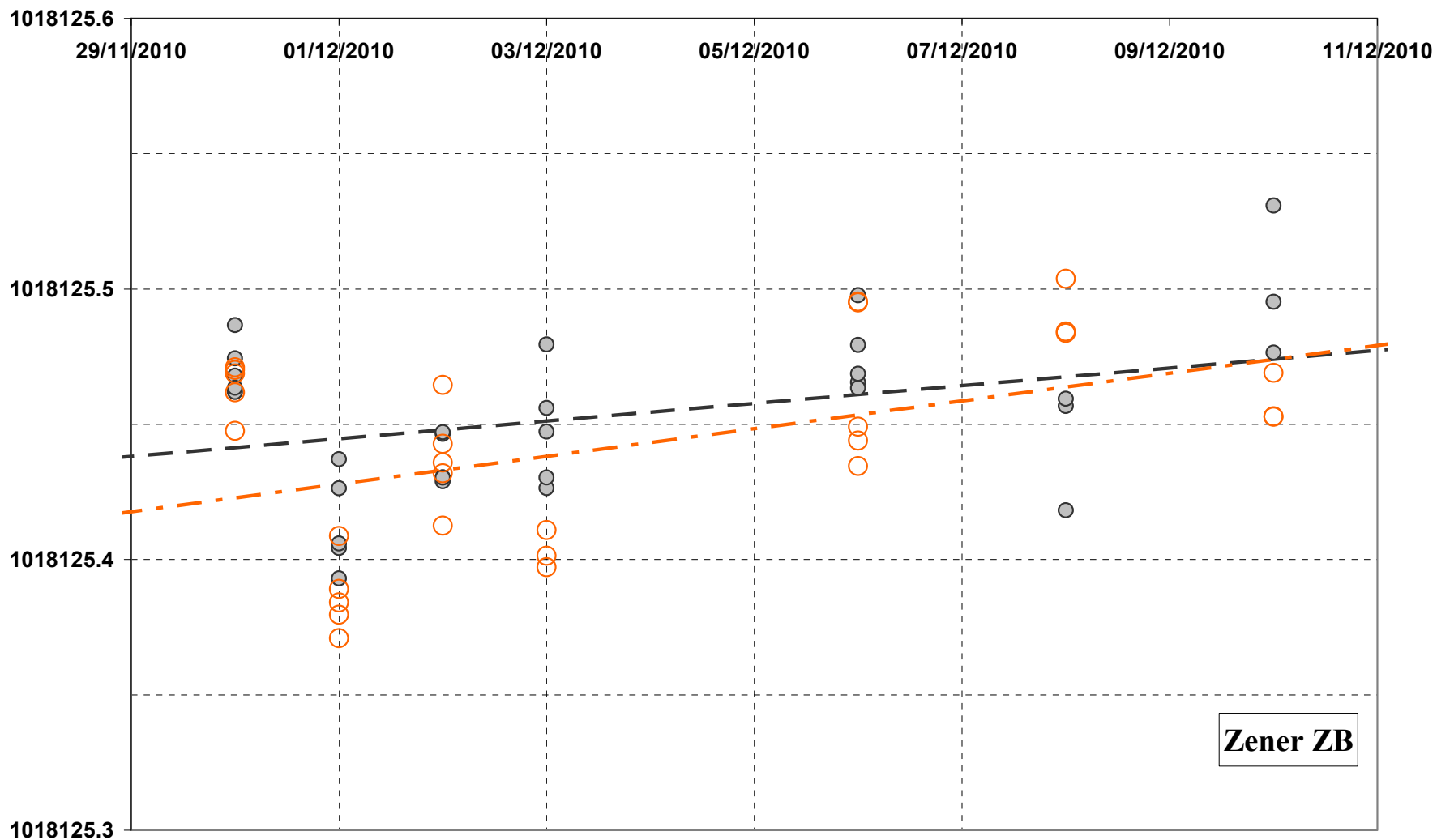


Fig. 12d : Day to day measurement result of ZB: the grey disks are the points obtained with the SINIS-based system and the open circles are the points obtained from the SIS-based system.

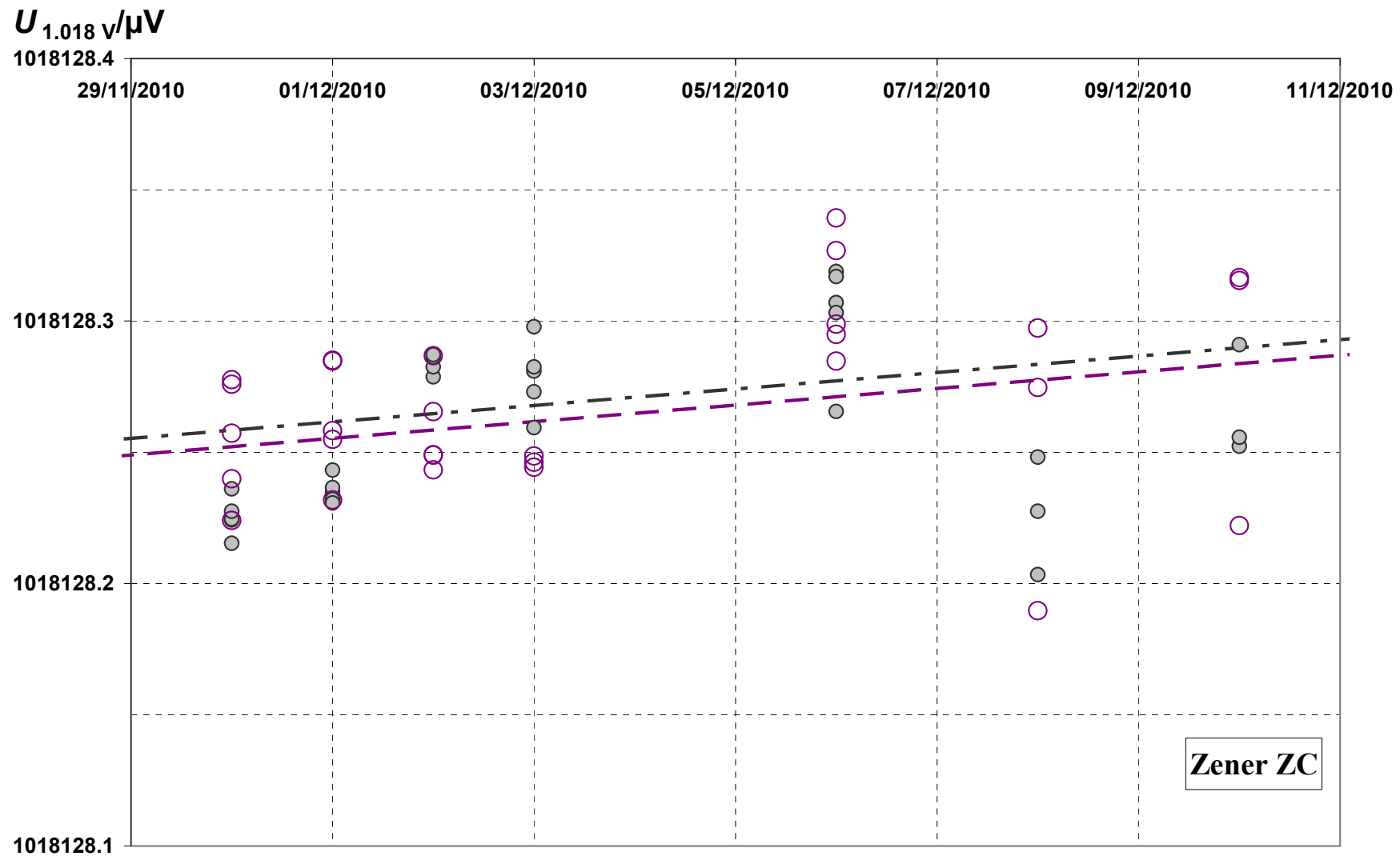


Fig. 12d : Day to day measurement result of ZC: the grey disks are the points obtained with the SINIS-based system and the open circles are the points obtained from the SIS-based system.

4.3 Comparison of the two set-ups through secondary voltage standards using a dedicated switch

In order to quickly evaluate two different JVS measurement systems in the same laboratory, it is possible to calibrate a secondary standard with each system and then compare the results. This method is used in direct, on-site Josephson voltage comparisons to investigate large discrepancies in the results [8]. A dedicated switch (BIPM Z switch) has been developed in the laboratory (Fig. 13) to rapidly measure two Zener standards with two different JVS measurement set-ups. The device allows the JVS systems to calibrate the two selected Zeners simultaneously. For example, while JVS system 1 is measuring Zener 1, JVS system 2 is measuring Zener 2 simultaneously. The Zeners are then “exchanged” between the two systems without removing any connection cables.

Moreover, during the measurement process, the polarity of the Zeners and the detectors are reversed using the switch. This allows the thermal electromotive forces to be cancelled out along the Zener measurement cable and to cancel out any detector offset and internal thermal electromotive forces, respectively.

In order to evaluate the performance of the “BIPM Z switch”, we performed measurements of TZS1 and TZS2 with the traditional JVS system (SIS array and an EM N1a nanovoltmeter) and with the new 1.018 V JVS associated with the new measurement set-up (SINIS array and a HP34420A nanovoltmeter) over a 10 day period. The complete series of results are presented in Figure 14a in terms of the absolute output voltage value of the Zener with respect to the measurement date. Figure 14b presents the same results in terms of the voltage difference measured by the two JVS set-ups for each Zener.

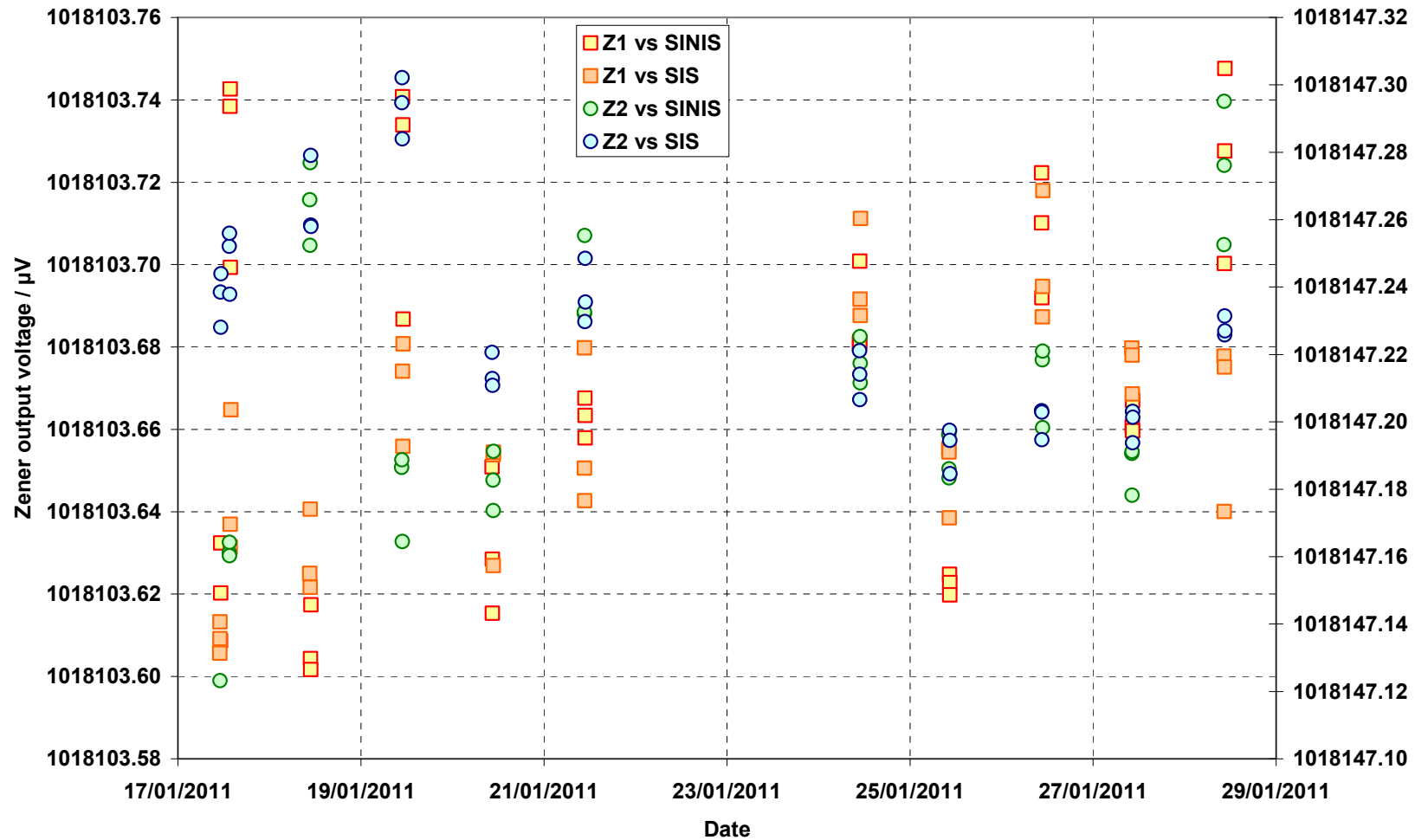


Fig. 14a : Day to day measurement results of TZS1 and TZS2 using alternatively two different JVS measurement set-ups with “BIPM Z switch”.
 The left Y-axis is dedicated to TZS1 output voltage scale and the right Y-axis to TZS2 output voltage scale.

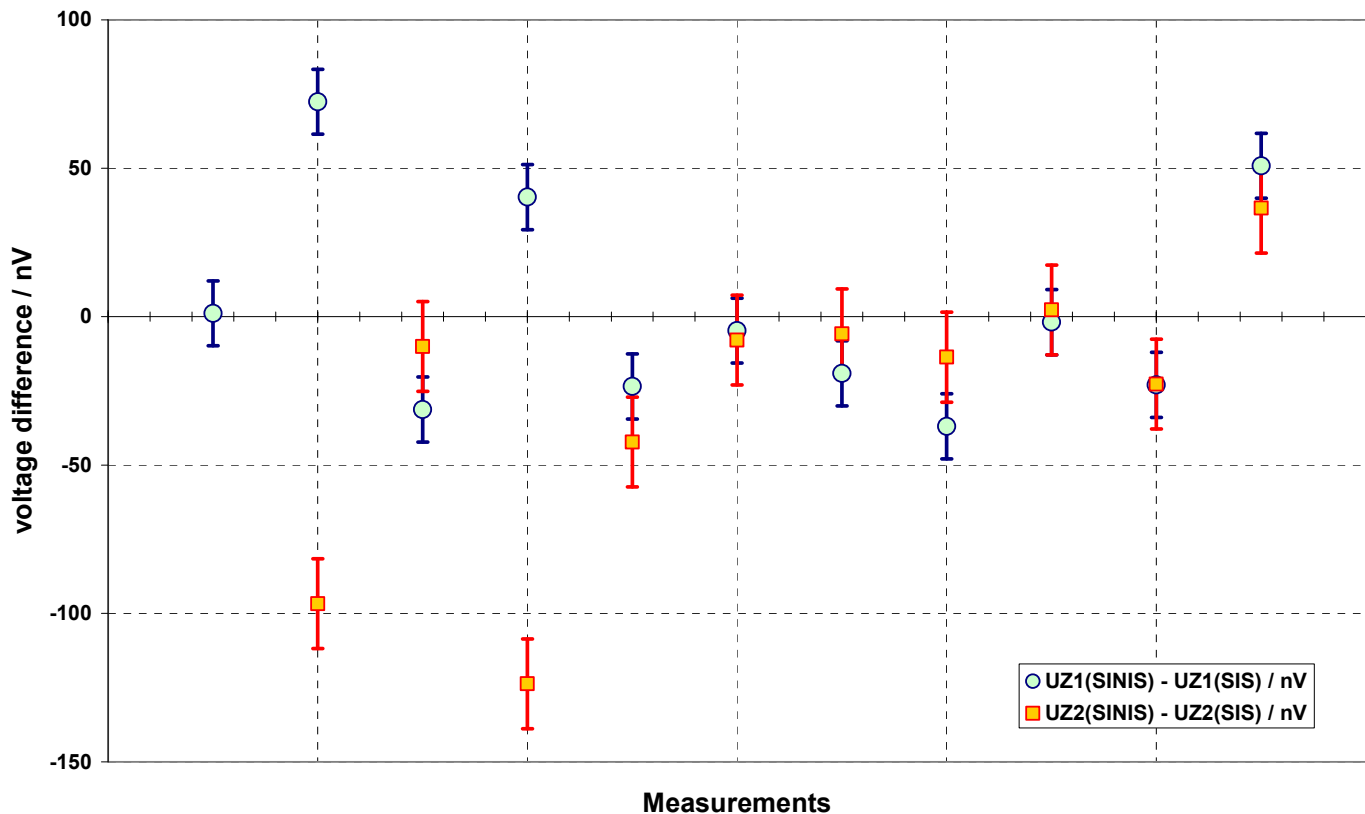


Fig. 14b : Day to day voltage difference $U_Z(\text{SINIS}) - U_Z(\text{SIS})$ of each standard (TZS1 in red and TZS2 in blue) using alternatively two different JVS measurement set-ups. The error bars represent the Type A uncertainty.

The results show that the two set-ups give similar results within the uncertainties. Note that the origin of the 3 discrepant values among the first four measurements was found in the loss of the frequency lock on the SIS JVS system. This experiment allows validation of the metrological quality of the "BIPM Z switch" to be operated during BIPM on-site Josephson comparisons (BIPM.EM-K10.a and b).

5 Conclusion

A new automated measurement set-up for calibrating Zener 1.018 V output voltage standards has been designed and built by the BIPM Electricity Department. This report presents the methodology followed to evaluate the performance of this new apparatus. The calibration results obtained with the new calibration set-up (based on a SINIS programmable array) and the previous set-up (based on a traditional SIS array) are equivalent within the stated uncertainties.

It is important to note that the new set-up is designed to minimize the voltage difference between the primary standard and the Zener to be calibrated. Therefore, an analogue detector can be used to measure the voltage difference

The first step of the evaluation process was to directly compare the two primary voltage standards using the SIS measurement set-up. The two standards were found to be in accordance within a total combined uncertainty of 11.7×10^{-10} V ($k=1$).

The second step consisted of comparing the results obtained with the two set-ups on five different Zener voltage standards. All these references were found to agree within a total combined uncertainty of 15 nV. The Type A uncertainty calculated from the standard deviation of the mean of the results was lower than the $1/f$ noise floor limit (typically 10 nV at 1 V) of the Zeners under test.

The final step consisted of repeating the second comparison using the “BIPM Z switch”. This device allows the JVS systems to calibrate the two selected Zeners simultaneously. In other words, while JVS system 1 is measuring Zener 1, JVS system 2 is simultaneously measuring Zener 2. The Zeners are then “exchanged” between the two systems without removing any connection cables.

Moreover, during the measurement process, the polarity of the Zener and the detector are reversed using the switch. Once again the results obtained are in very good agreement with the stated uncertainties.

All the results converge and confirm that the new automated measurement set-up is operational in the sense that it is consistent with the previous set-up and that the traceability of the results to the primary JVS can be guaranteed. Extension of the set-up to the 10 V level will be possible as soon as 10 V programmable arrays become available. Only a few modifications related to the biasing current intensity will be required.

References

- [1] Solve S, Chayramy R and Reymann D 2007 A new fully automated measurement chain for electronic voltage standards at 1.018 V [*IEEE Trans. Instrum. Meas.* **56** 588–591](#)
- [2] Reymann D 1991 A Practical Device for 1-nV Accuracy Measurements with Josephson Array, [*IEEE Transactions on Instrumentation and Measurement* **40**\(2\) 309–311](#)
- [3] Schulze H *et al* 1999 SINIS Josephson junctions for programmable voltage standards *Appl. Phys. Lett.* **73** 996–998
- [4] Solve S and Chayramy R, A very low Thermal Electromotive Forces scanner, to be submitted.
- [5] Dutkiewicz J *et al* 1989 The Cd-Sn (Cadmium-Tin) System, *Bulletin of Alloy Phase diagrams*, **10** (3) 223–229
- [6] Witt T J 2005 Allan Variances and Spectral Densities for DC Voltage Measurements With Polarity Reversals, [*IEEE Trans. Instrum. Meas.* **54** 550–553](#)
- [7] On-site direct BIPM Josephson comparisons (BIPM.EM-K10.b) reports available from <http://kcdb.bipm.org>
- [8] Solve S *et al* 2010 Comparison of the Josephson voltage standards of the EIM and the BIPM [*Metrologia* **47** 01009](#)

DISCLAIMER

Certain commercial equipment, instruments or materials are identified in this paper in order to adequately specify the environmental and experimental procedures. Such identification does not imply recommendation or endorsement by the BIPM, nor does it imply that the materials or equipment identified are necessarily the best available for the purpose.